Enhancement of a robust arcuate GABAergic input to gonadotropin-releasing hormone neurons in a model of polycystic ovarian syndrome

Aleisha M. Moore, Mel Prescott, Christopher J. Marshall, Siew Hoong Yip, and Rebecca E. Campbell[1]

Centre for Neuroendocrinology and Department of Physiology, School of Medical Sciences, University of Otago, Dunedin, 9054, New Zealand

Polycystic ovarian syndrome (PCOS), the leading cause of female infertility, is associated with an increase in luteinizing hormone (LH) pulse frequency, implicating abnormal steroid hormone feedback to gonadotropin-releasing hormone (GnRH) neurons. This study investigated whether modifications in the synaptically connected neuronal network of GnRH neurons could account for this pathology. The PCOS phenotype was induced in mice following prenatal androgen (PNA) exposure. Serial blood sampling confirmed that PNA elicits increased LH pulse frequency and impaired progesterone negative feedback in adult females, mimicking the neuroendocrine abnormalities of the clinical syndrome. Imaging of GnRH neurons revealed greater dendritic spine density that correlated with increased putative GABAergic but not glutamatergic inputs in PNA mice. Mapping of steroid hormone receptor expression revealed that PNA mice had 59% fewer progesterone receptor-expressing cells in the arcuate nucleus of the hypothalamus (ARN). To address whether increased GABA innervation to GnRH neurons originates in the ARN, a viral-mediated Cre-lox approach was taken to trace the projections of ARN GABA neurons in vivo. Remarkably, projections from ARN GABAergic neurons heavily contacted and even bundled with GnRH neuron dendrites, and the density of fibers apposing GnRH neurons was even greater in PNA mice (56%). Additionally, this ARN GABA population showed significantly less colocalization with progesterone receptor in PNA animals compared with controls. Together, these data describe a robust GABAergic circuit originating in the ARN that is enhanced in a model of PCOS and may underpin the neuroendocrine pathophysiology of the syndrome.

GnRH | PCOS | GABA | progesterone receptor | luteinizing hormone

Gonadotropin-releasing hormone (GnRH) neurons, located in the hypothalamus, control fertility by driving the secretion of the gonadotrophins, luteinizing hormone (LH), and follicle-stimulating hormone (FSH) from the pituitary gland. The pulse amplitude and frequency of LH and FSH shape the sequence of events that occur at the ovary, including follicular development, gonadal steroid synthesis, and ovulation. Hormones secreted from the ovary, in turn, provide critical feedback signals to GnRH neurons through a network of hormone-sensitive neurons. Gonadal hormone feedback directs both the firing of GnRH neurons and pulsatile release of the GnRH peptide (1).

Polycystic ovarian syndrome (PCOS), the most common form of anovulatory infertility (2), is estimated to affect more than 100 million women worldwide (3). Most women diagnosed with PCOS exhibit increased LH pulse frequency and decreased FSH release, suggestive of rapid GnRH pulse frequency (4). High LH, in turn, contributes to increased androgen production from ovarian theca cells, whereas decreased FSH disrupts follicle maturation and ovulation. Elevated GnRH/LH secretion in women with PCOS is less responsive to exogenous estrogen and progesterone (P4) administration (5, 6), suggesting that steroid hormone negative feedback to GnRH neurons is impaired. In animal models, elevated androgens are associated with blunted P4 negative feedback in particular (7, 8).

Although the origin of GnRH/LH hypersecretion in PCOS is unknown, impaired steroid hormone negative feedback may lie within the hormone-sensitive afferent neuronal network to GnRH neurons. Identifying the specific neuronal elements affected is challenging in women; however, discoveries can be made in animal models (9, 10). PCOS is most commonly modeled through exposure to androgens during critical periods of development (11). Women exposed to elevated prenatal androgens (PNAs) develop the cardinal reproductive and endocrine features of PCOS in adulthood (12, 13), and PNA treatment produces a PCOS-like phenotype in all mammalian species studied to date (11). In the mouse, PNA elicits many of the key neuroendocrine features of the syndrome, suggestive of impaired steroid hormone feedback to the GnRH pulse generator (14, 15), however, it remains to be determined directly whether P4 negative feedback and LH pulse frequency are modified.

P4 modulation of GnRH neurons via classical progesterone receptors (PRs) is most likely transsynaptic, as GnRH neurons do not express PRs. Many P4-sensitive populations have been identified throughout the hypothalamus, including neurons expressing gamma-aminobutyric acid (GABA) (16), glutamate (17), and various neuropeptides (18, 19). Both endogenous GnRH neuron firing activity and GABAergic postsynaptic currents are increased in PNA mice (15, 20). However, the specific P4-sensitive neuronal phenotype that relays feedback signals to GnRH neurons is so far unknown. The aim of the present study was to characterize whether LH pulse frequency and P4 negative feedback are impaired in a mouse model of PCOS and to investigate what modifications exist in the GnRH neuronal network that may impair negative feedback.

Significance

Polycystic ovarian syndrome (PCOS) is the leading cause of anovulatory infertility. Although the etiology of PCOS is unclear, disrupted central mechanisms mediating steroid hormone feedback to gonadotropin-releasing hormone (GnRH) neurons have been suggested. We describe here, in a mouse model reflecting the clinical neuroendocrine phenotype of PCOS, evidence for disordered progesterone (P4)-sensitive GABAergic input to GnRH neurons, originating specifically within the arcuate nucleus. These discoveries define a previously unidentified neuronal pathway, potentially critical for the steroid hormone feedback control of fertility. Of clinical relevance, our findings help explain the impact of GABA agonist drugs on menstrual cycle irregularity and interference with oral contraceptives and could be the basis for understanding clinical therapies of PCOS.

Results

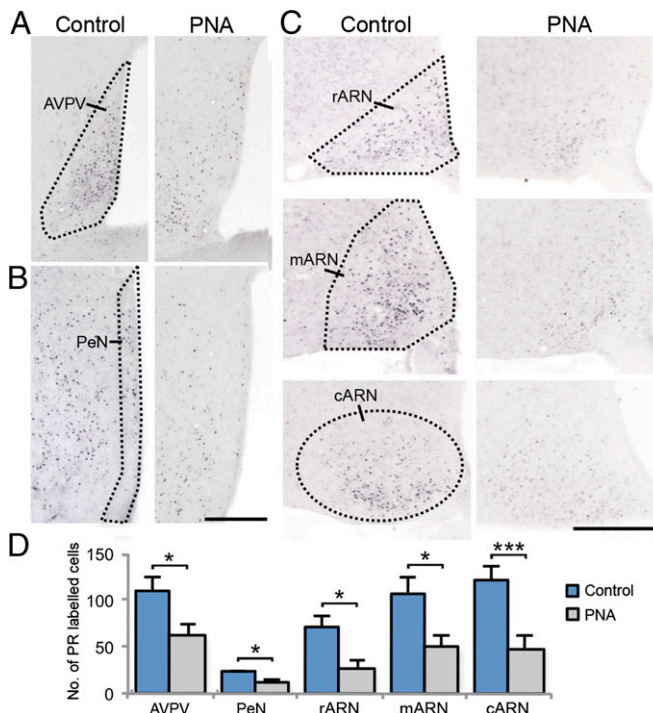**PNA Mice Exhibit the Cardinal Neuroendocrine Features of PCOS.** LH pulses, identified by peak values greater than 3 SDs above baseline and shape, were measured in serial blood samples from gonadally intact mice. Compared with diestrus controls, PNA mice had significantly increased LH pulse frequency (Fig. 1, $P <$ 0.05), with a significantly reduced pulse interval (62 ± 5.8 vs. 41 ± 4.9 min, $P < 0.05$). Mean LH pulse amplitude was significantly decreased in PNA mice (Fig. S1A, $P < 0.05$), and the mean LH baseline and area under the curve were not different between groups (Fig. S1 B and C). PNA mice had significantly elevated plasma testosterone levels compared with controls ($P < 0.05$); however, serum estradiol and plasma P4 levels were not significantly different between groups (Fig. S2). P4 negative feedback was assessed in control and PNA mice by measuring the post-castration rise in plasma LH levels and the response to P4 feedback by exogenous administration of a P4 pellet (Fig. 1D). The basal concentration of LH measured before ovariectomy (OVX) at a single time point was not different between groups. Three days following OVX, LH was significantly elevated in both control ($P < 0.001$) and PNA ($P < 0.01$) mice. P4 replacement for 48 h significantly decreased LH levels in control mice ($P < 0.05$) but had no effect on LH levels in PNA mice. Faster LH pulsatility and the absence of a negative feedback response to P4 indicate that the PNA mouse model mimics the neuroendocrine features of PCOS.

PR Expression in Specific Hypothalamic Nuclei Is Reduced in PNA Mice. Steroid hormone receptors for estrogen, P4, and androgen were mapped throughout the hypothalamus and quantified in specific hypothalamic areas previously identified to contain afferents to GnRH neurons (21). PNA treatment significantly decreased the number of PR-positive cells within the anteroventral periventricular nucleus (AVPV; $P < 0.05$, Fig. 2A), periventricular nucleus (PeN; $P < 0.05$, Fig. 2B), and the rostral ($P < 0.05$), middle ($P < 0.05$), and caudal ($P < 0.001$) regions of the arcuate nucleus (ARN) (Fig. 2C), representing a 44.0%, 49.5%, and 58.3% decrease in PR-expressing cells within these areas, respectively (Fig. 2D). The number of ERα-positive cells was unchanged by PNA treatment in the AVPV and ARN; however, ERα expression was significantly increased (45.7%) in the PeN of PNA mice compared with controls ($P < 0.01$, Fig. S3 A and B). The number of AR-positive cells was higher in the AVPV of PNA mice compared with controls ($P < 0.05$, 31.1%) but unchanged in the PeN and ARN (Fig. S3 C and D). These data illustrate that the
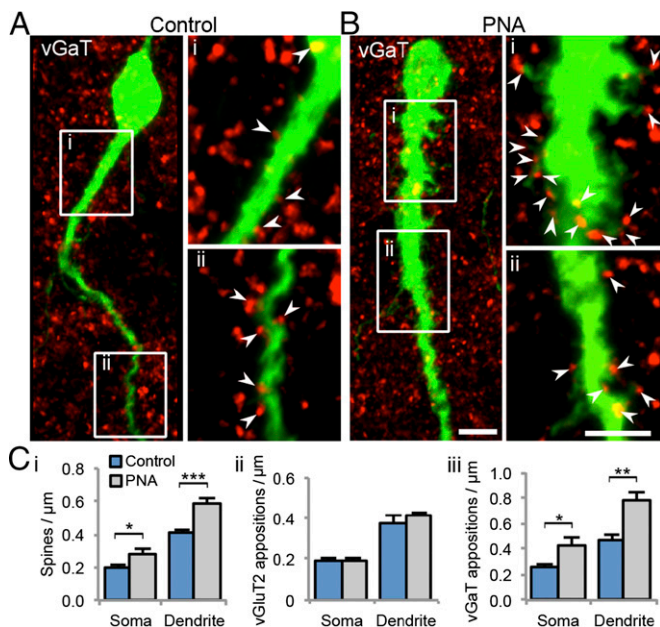

Fig. 2. PR immunoreactivity in representative unilateral sections containing the AVPV (outlined, A), PeN (outlined, B), and ARN (outlined, C) in control ($n = 7$) and PNA ($n = 7$) mice. (Scale bar, 250 μm.) (D) The number of PR-labeled cells is significantly decreased in PNA mice compared with controls.

expression of all three steroid receptors are abnormal in PCOS mice, with PR being the most widely affected.

GnRH Neurons in PNA Mice Have Increased Spine Density Correlating with Greater GABAergic, but Not Glutamatergic, Synaptic Contact. Although P4 modulation of GnRH activity can occur through diverse mechanisms (22), classical PR-mediated regulation of negative feedback to GnRH neurons is most likely via an afferent neuronal network (23). In PNA and control GnRH-GFP mice, afferent synaptic inputs to GnRH neurons were investigated by quantifying GnRH neuron spine density and close apposition with vesicular glutamate transporter 2 (vGluT2)-immunoreactive (ir) puncta (Fig. S4) and vesicular GABA transporter (vGaT)-ir puncta (associated with synaptic terminals) (Fig. 3). GnRH neuron spine density was significantly greater at both the soma ($P < 0.05$) and proximal dendrite ($P < 0.001$) in PNA mice compared with controls (Fig. 3 C, i). Spine number was significantly increased in PNA mice out to 60 μm along the extent of the primary dendrite (Fig. S5A). The density (Fig. 3 C, ii) and number (Fig. S5B) of closely apposed vGluT2-ir puncta (Fig. 3 C, ii) with GnRH neurons at the soma and dendrite were not different between control and PNA mice despite the observed increase in spine density. No significant differences in the percentage of spines apposed by one or more vGluT2-ir puncta (Fig. S6 A and C) were observed. However, the density of closely apposed vGaT-ir puncta with GnRH neurons was significantly higher at the soma ($P < 0.05$) and dendrite ($P < 0.01$) in PNA mice (Fig. 3 C, iii), evident within the first 60 μm of the dendrite (Fig. S5C). In addition to an increased absolute number of GABAergic contacts, the percentage of somatic ($P < 0.05$) and dendritic ($P < 0.01$) spines apposed by one or more vGaT contacts was significantly increased in PNA mice (Fig. S6 B and D). Together, these data identify anatomical evidence for modified afferent synaptic input to GnRH neurons in PNA mice, including increased GnRH neuron spine density that correlates not with glutamate input but with increased putative GABAergic innervation.

Fig. 1. LH concentrations from representative control (A, $n = 14$) and PNA (B, $n = 19$) mice. Stars indicate LH pulses. (C) PNA treatment significantly increases LH pulse frequency. (D) LH concentrations from control ($n = 6$) and PNA ($n = 8$) mice sampled at three time points: intact, 3 d after OVX, and 48 h postprogesterone pellet implantation.

Moore et al.

www.manaraa.com

Fig. 3. Projected confocal images (8-μm optical thickness) of GnRH neurons (green) closely apposed by vGaT-ir puncta (red) from control (*A*, n = 5) and PNA (*B*, n = 5) mice. (*i* and *ii*) Projected confocal images (1.35-μm optical thickness) of the GnRH neuron dendrite from corresponding white boxes. Arrowheads indicate points where vGaT-ir puncta are considered to contact the GnRH neuron. (Scale bar, 5 μm.) (*C*) The density of GnRH neuron spines (*i*), vGluT2-ir puncta closely apposed to GnRH neurons (*ii*), and vGaT-ir puncta closely apposed to GnRH neurons (*iii*) from control and PNA mice.

GnRH Neurons Are Robustly Contacted by GABA Neurons Originating in the ARN.

The ARN is known to be important for negative feedback (24) and contain GABAergic neurons (25). The marked reduction in PR expression in the ARN found here led us to hypothesize the ARN as a potential origin of increased GABAergic innervation to GnRH neurons. ARN GABA neuron projections were targeted by injecting an adenoviral vector expressing farnesylated enhanced green fluorescent protein (Ad-iZ/EGFPf) into the ARN of vGaT-Cre mice (Fig. 4*A* and Fig. S7*A*), where the farnesyl sequence targets the EGFP to the membrane of the cell (Fig. S7*B*). The average number of EGFPf-positive GABAergic neurons in the rostral, middle, and caudal regions of the ARN was not significantly different between control and PNA mice (Fig. S7*C*). In control mice (Fig. 4*B*), ARN GABAergic projections densely contacted the majority of GnRH neurons within the medial septum (MS; 55.0 ± 8.1%), rostral preoptic area (rPOA; 66.5 ± 8.4%), and anterior hypothalamic area (70 ± 10.5%). Similarly, in PNA mice (Fig. 4*C*), ARN GABAergic fibers closely apposed 46.7 ± 15.7% of MS GnRH neurons, 65 ± 10.5% of rPOA GnRH neurons, and 66.7 ± 12.2% of anterior hypothalamic area GnRH neurons. ARN GABAergic fibers contacted GnRH neurons at single points, formed multiple contacts along the soma and dendrites, or even bundled with GnRH neuron dendrites (Fig. 5*A*).

ARN GABAergic Innervation of GnRH Neurons Is Even More Pronounced in PNA Mice.

The density of ARN GABA fibers contacting the soma of GnRH neurons was not different between control (0.05 ± 0.01 fibers per μm) and PNA (0.05 ± 0.01 fibers per μm) mice. However, PNA mice exhibited a significantly higher density of ARN GABA fibers contacting the dendrite (0.08 ± 0.01 fibers per μm) compared with controls (0.04 ± 0.01 fibers per μm; $P < 0.05$, Fig. 5*B*). Although the number of GnRH neurons contacted by ARN GABA fibers was not different between groups, the number of fibers contacting the dendrites of GnRH neurons was increased in PNA mice compared with controls ($P <$

0.05, Fig. 5*C*) and was greatest within the first 30 μm of the proximal dendrite (Fig. 5*D*). Of the GnRH neurons contacted by ARN GABAergic fibers, the percentage contacted at a single point was significantly higher in control mice compared with PNA mice (Fig. 5*E*). GABA neurons in the dorsomedial nucleus of the hypothalamus (DMH) were also filled and traced (Fig. S8*A*, n = 4). Although ∼65% of the GnRH neuron population was contacted by GABA neurons originating in the ARN, only 10 ± 0.7% of GnRH neurons received any GABAergic fiber contact from DMH neurons. The density of DMH GABAergic fibers contacting the GnRH neuron soma and dendrite was markedly lower, at 0.017 ± 0.009 apposing fibers per μm and 0.022 ± 0.006 apposing fibers per μm, respectively (Fig. S8*B*).

ARN GABA Neurons Express PR and Show a Significant Decrease in PR Expression in PNA Mice.

To evaluate whether the decreased PR expression identified in the ARN of PNA mice was specific to GABA neurons, PR coexpression with EGFPf-filled GABA neurons was quantified. Coexpression of PR in GABA neurons was present in the rostral (47.0 ± 2.6%), middle (47.9 ± 5.8%), and caudal (40.3 ± 6.1%) regions of the ARN in control mice (Fig. 6*A*). In contrast, although GABA neuron number was not different between groups, the percentage of GABA neurons coexpressing PR was significantly reduced in the rostral (30.3 ± 4.1%, $P < 0.05$), middle (25.5 ± 5.3%, $P < 0.05$), and caudal (15.7 ± 4.6%, $P < 0.05$) regions of the ARN in PNA mice (Fig. 6 *B* and *C*).

Discussion

These findings reveal a brain pathway within the GnRH neuronal network potentially underpinning the neuroendocrine abnormalities of PCOS. Using a mouse model of PCOS, shown here to exhibit the cardinal neuroendocrine features of the syndrome, we find that GnRH neurons possess elevated spine density and an increased density of putative GABAergic inputs. GABA neurons originating in the ARN were discovered to strongly project to GnRH neurons in controls and provide even more robust contact to GnRH neurons in PCOS-like mice. ARN GABA neurons with identified projections to GnRH neurons were additionally found to express PRs in fertile controls and exhibit a marked reduction in this coexpression in the P4-insensitive PCOS-like mice. These observations suggest that ARN GABA neurons are a functionally relevant component of the GnRH neuronal network and that altered ARN GABA neuron inputs to GnRH neurons contribute to the neuroendocrine dysfunction of PCOS.

To make meaningful progress in dissecting out altered neuronal function in PCOS, an appropriate model of the syndrome
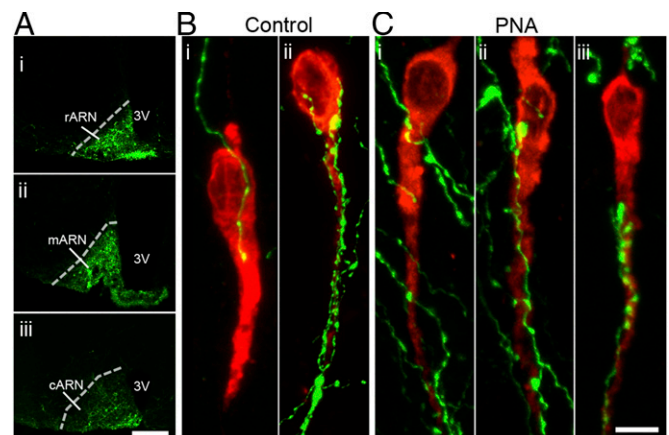
Fig. 4. (*A*) A single injection of Ad-iZ/EGFPf induces EGFPf expression in GABAergic neurons of the rostral (*i*), middle (*ii*), and caudal (*iii*) regions of the ARN. (Scale bar, 0.5 mm.) GnRH neurons (red) from control (*B*, n = 6) and PNA (*C*, n = 6) mice closely apposed by ARN GABAergic fibers (green). (Scale bar, 5 μm.) 3V, third ventricle.

Moore et al.

www.manaraa.com
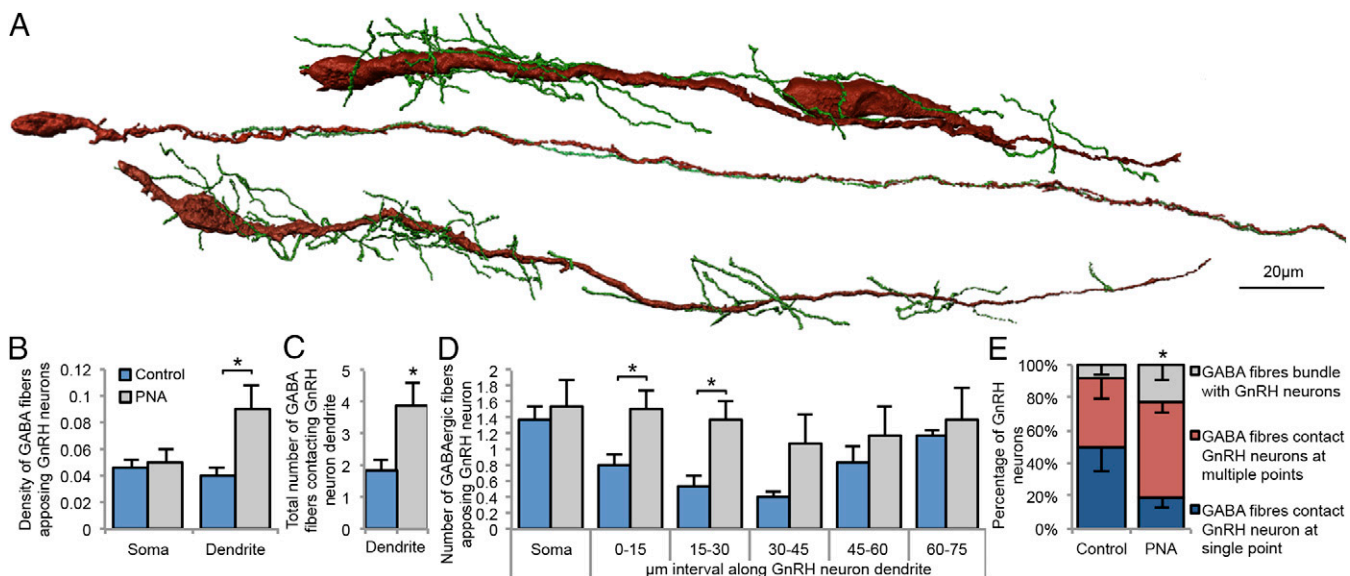
Fig. 5. (*A*) Reconstructions using AMIRA software illustrating the robust degree of contact between ARN GABAergic fibers (green) and the lengthy dendrites of GnRH neurons (red). The density (*B*) and total number (*C*) of closely apposed fibers from ARN GABAergic neurons to GnRH neurons is significantly increased at the dendrite of PNA (*n* = 6) mice compared with controls (*n* = 6). (*D*) The number of ARN GABAergic fibers closely apposed to GnRH neurons is significantly increased along the first 30 μm of the GnRH neuron dendrite. (*E*) The percentage of GnRH neurons that are contacted by ARN GABAergic fibers at a single point is significantly decreased in PNA mice compared with controls.

is essential. The PNA mouse model elicits a phenotype that possesses the majority of the reproductive deficits seen in the clinic, including hyperandrogenism, disrupted estrous cyclicity, and modified ovarian morphology (14, 15, 26), but reflects only minor metabolic disturbances (27), suggesting that this model is most representative of the "lean PCOS phenotype" (28). Women with PCOS present with a reduced ability for estrogen and P4 to slow the GnRH/LH pulse generator (6). The PNA mouse model possesses a small elevation in basal plasma LH levels (15), impaired estrogen negative feedback (14), and increased GnRH neuron firing activity (20) in support of similar impairments in negative feedback. However, until now, it has been challenging to examine LH pulsatility, a proxy for GnRH pulsatiliy and the only meaningful way to examine the speed of the GnRH/LH pulse generator. Using a sensitive ELISA to measure LH in very small volumes of whole blood (29), we show that LH pulse frequency is significantly increased in the PNA mouse. This may be due in part to impaired estrogen negative feedback (14), but we also show here that P4 is unable to blunt a post-OVX rise in LH in PNA mice, suggesting that P4 negative feedback is equally impaired. As commonly seen in animal models in which the circuitry regulating steroid hormone feedback is affected (24, 30), the post-OVX rise was attenuated in PNA mice compared with controls. This suggests that other changes in the regulation of the basal activation of GnRH neurons may be altered, due to either the initial programming effects of PNA exposure or the subsequent loss of steroid hormone sensitivity.

Although rodent species lack a true luteal phase, PRs are required for normal cycling and fertility in mice, and evidence suggests that progesterone may contribute to negative feedback suppression of LH (31). Mapping of the steroid hormone receptors ERα, PR, and AR revealed a dramatic decrease in the number of cells expressing PR in the ARN and RP3V of PNA mice. Reduced P4 sensitivity was most dramatic within the ARN, with a nearly 60% decrease in PR-positive cells. This finding is in line with previous work showing decreased PR mRNA within the hypothalamus of PNA rats (32) and the ARN of PNA ewes (33). Although the mechanism of reduced PR expression remains to be determined, we can rule out reduced estrogen or P4 levels, as these remain unchanged in PNA mice.

In addition to identifying regions where hormone insensitivity may originate, we also investigated whether abnormalities in direct inputs to GnRH neurons could be identified. Using GnRH-GFP mice (34), we identified increased spine density in PNA mice. Spines in other neuronal phenotypes are a correlative measure of excitatory, predominantly glutamatergic, input (35). However, the density of vGluT2 appositions to GnRH neuron somata and dendrites directly onto spines was unchanged, suggesting that GnRH neuron spine changes are not necessarily related to changes in glutamatergic input. Interestingly, the increase in spine density did correlate with increased GABAergic appositions with GnRH neurons, including an increase in the percentage of GnRH neuron spines contacted by vGaT-ir puncta. These data are compatible with previous findings showing increased GABAergic postsynaptic currents in PNA mice (15). Although principally recognized as an inhibitory neurotransmitter in the adult brain, there is now a consensus that GABA acts through GABA_A receptors to activate adult GnRH neurons (36). Therefore, the current data suggest a mechanism by which elevated GABAergic innervation of GnRH neurons increases GnRH/LH pulse frequency in a PCOS-like state.

Both animal and human studies support GABAergic network involvement in interfering with P4 negative feedback to GnRH neurons (7, 37, 38). Drugs that enhance GABA activity, such as those used to treat epilepsy, can interfere with the activity of progestogen containing oral contraceptives (38) and even elicit the onset of PCOS (39). We have now identified a P4-sensitive GABAergic network residing specifically within the ARN potentially mediating these disruptions. In rodent species, the ARN has been demonstrated to be essential for pulsatile LH release (40), estrous cyclicity (24), and estradiol negative feedback regulation of GnRH neurons (41). Likewise, in the ewe, the ARN plays a major role in mediating P4 negative feedback to GnRH neurons (42), predominantly through dynorphin and kappa opioid receptor actions (43). Interestingly, the number of dynorphin, neurokinin B, and PR-positive cells are significantly reduced in the ARN of PNA ewes (33).

Using viral-mediated in vivo "filling," we have revealed a robust projection to GnRH neurons from ARN GABA neurons. As we have only filled a subset of ARN GABA neurons and visualized only the proximal portion of the GnRH neuron, we

Moore et al.

NEUROSCIENCE

www.manaraa.com
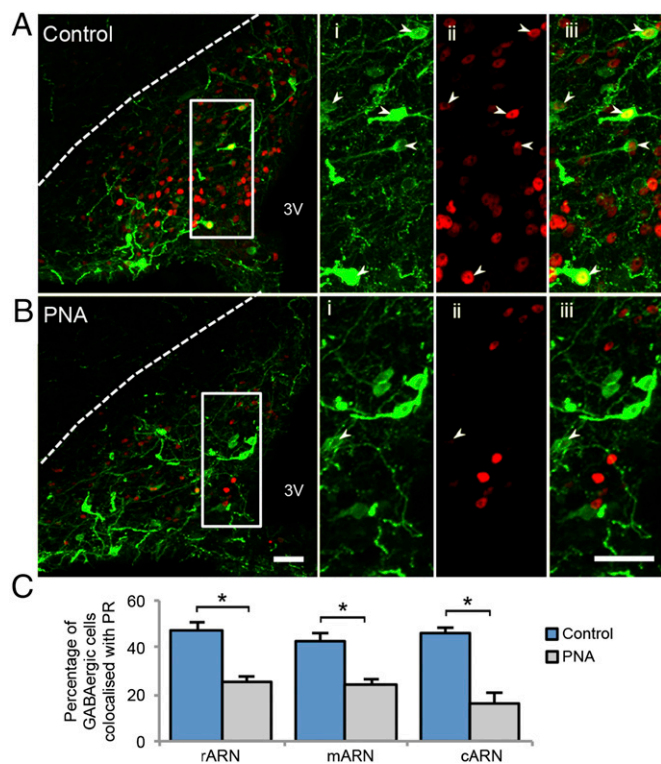
Fig. 6. Projected confocal images of EGFPf-positive GABA neurons and PR-positive nuclei in the ARN of control (*A*, *n* = 4) and PNA (*B*, *n* = 5) mice. High-magnification images of EGFPf-positive GABAergic neurons (*i*), PR-positive nuclei (*ii*), and merged images (*iii*) from corresponding white boxes. Arrows indicate ARN GABAergic cells that are colocalized with nuclear PRs. (Scale bars, 50 μm.) (*C*) The percentage of GABAergic cells colocalized with PRs is significantly decreased in the rostral, middle, and caudal ARN of PNA mice compared with controls. 3V, third ventricle.

are likely underestimating the prevalence of this innervation. ARN GABAergic contacts were observed to terminate on the GnRH neuron somata, along the entire visible extent of the GnRH neuron dendrite, and even bundle with a subpopulation of GnRH neurons in a vertical-type orientation. GnRH neuron dendrites have been previously shown to bundle and receive shared synaptic contacts of an unknown phenotype (44). The close association between ARN GABAergic fibers and GnRH neuron dendrites found here raises the question of whether these shared inputs may be GABAergic terminals from neurons originating in the ARN. The peptidergic phenotype of the ARN GABA neurons that project to GnRH neurons remains to be determined in future studies.

Arcuate GABA input to GnRH neurons was even greater in PNA mice, and ARN GABA neurons exhibited significantly reduced PRs. These data suggest that at least some of the increased GABA contact to GnRH neurons is originating from the ARN and might mediate impaired P4 sensitivity in the hypothalamus of PNA mice. Impaired P4 feedback in the ARN could lead to enhanced GABA signaling at the GnRH neuron that is predominantly responsible for the increase in LH pulse frequency that subsequently drives hyperandrogenism and disrupted estrous cyclicity in this mouse model of PCOS. These observations highlight ARN GABA neurons as a functionally relevant component of the GnRH neuronal network that contributes to the neuroendocrine dysfunction of PCOS and highlight a potential mechanism mediating the effects of GABA-modulating drugs on female reproductive health.

Materials and Methods

Animals. Adult female C57BL/6J (B6) wild-type, GnRH-GFP (45), and vGaT-Cre (25) mice, 60–80 d of age, were housed with ad libitum access to food and

water. All protocols were approved by the University of Otago Animal Ethics Committee (Dunedin, New Zealand). PNA treatment as described previously (14) was used to model PCOS.

Pulsatile LH Measurements. Control (*n* = 14) and PNA (*n* = 19) mice were habituated with daily handling for 4 wk. As previously reported (29), 4 μL blood samples were taken from the tail in 6- or 10-min intervals for 2 h (between 12:00 and 15:00), diluted in PBS-Tween, and immediately frozen. LH levels were determined by sandwich ELISA (29). The intraassay coefficient of variation was 3.66%, and the interassay coefficient of variation was 11.7%. Pulses were confirmed using DynPeak (46).

Progesterone Negative Feedback Trial. Control (*n* = 8) and PNA (*n* = 7) mice were anesthetized with a Ketamine (75 mg/kg) and Domitor (1 mg/kg) mixture (s.c.) before tail blood sampling and bilateral OVX. Anesthesia was lifted by Antisedan (1 mg/kg, s.c.). Three days later, anesthesia and tail-tip bleeding were performed to determine post-OVX LH concentrations. Before anesthesia was reversed, all mice were implanted with a time-release P4 pellet (0.12 mg of P4 per day) to mimic mouse estrous levels of P4 (Innovative Research of America) (37). Forty-eight hours later, mice received an i.p. injection of pentobarbital (3 mg/100 μL), and blood was drawn from the inferior vena cava. LH concentration was determined by sandwich ELISA. The intraassay coefficient of variation was 3%.

ELISA. LH levels were determined by a sandwich ELISA as described previously (29) using the mouse LH–RP reference provided by A. F. Parlow (National Hormone and Pituitary Program, Torrance, CA). Commercially available ELISA kits were used to measure levels of plasma testosterone (Demeditec Diagnostics, GmnH), serum estradiol (Calbiotech), and plasma P4 (Cayman Chemical Co.) according to the manufacturers' instructions. The intraassay coefficient of variation for testosterone, estradiol, and P4 was 9.01%, 12.04%, and 9.3%, respectively.

Intracerebral Injections. Control (*n* = 6) and PNA (*n* = 6) mice were anesthetized with isoflurane and placed in a stereotaxic frame (Stoelting). A small hole was drilled in the skull 1 mm posterior to Bregma and 0.3 mm lateral to midline, and a cannula containing 250 nL of Ad-iZ/EGFPf from a 5.1×10^{11} pfu/mL stock (virus gifted by M. G. Myers Jr., University of Michigan, Ann Arbor, MI) was lowered 6.1 mm ventral to dura. After 3 min, Ad-iZ/EGFPf was injected into the ARN at a rate of 20 nL/min. After an additional 5 min, the syringe was removed and the skin closed with sutures. The injected brains were collected from diestrus mice 7–12 d following injection.

Immunohistochemistry. All mice underwent transcardial perfusion with paraformaldehyde (4%) during diestrous. Perfusion fixed brains were removed, postfixed for 1 h at room temperature, saturated in 30% sucrose made up in Tris buffer saline solution overnight, and cut into 30-μm-thick coronal sections using a freezing microtome. Free-floating immunohistochemistry was performed as previously reported, with primary antibody omission serving as a negative control (14, 34). The following primary antibodies were used: polyclonal rabbit anti-GFP (1:5,000, Invitrogen), polyclonal chicken anti-GFP (1:5,000, Aves Labs Inc.), polyclonal rabbit anti-vGluT2 and polyclonal rabbit anti-vGaT (1:750, Synaptic Systems), polyclonal rabbit anti-PR (Chromagen label, 1:2,000; immunofluorescent label, 1:250; DAKO Corp.), rabbit anti-estrogen receptor alpha (ERα, 1:10,000, Millipore), polyclonal rabbit anti-androgen receptor (AR, PG-21, 1:500, Millipore), and guinea pig anti-GnRH (1:5,000, gift from Greg Anderson, University of Otago, Dunedin, New Zealand). The following secondary antibodies were used: biotinylated goat anti-rabbit and biotinylated goat anti-guinea pig (1:200, Vector Laboratories Inc.) and goat anti-rabbit AlexaFluor568, goat anti-guinea pig AlexaFluor568, goat anti-rabbit AlexaFluor488, goat anti-chicken AlexaFluor488, and streptavidin 568 (1:200, Molecular Probes, Invitrogen).

Image Analysis. Light microscopy image acquisition was performed using an Olympus Bx-51 (Olympus Optical) or a Zeiss LSM710 confocal microscope with an argon laser exciting at 488 nm and a helium laser exciting at 543 nm.

Quantification of steroid hormone receptor-positive nuclei in control and PNA mice was performed in two representative sections from each nucleus analyzed. Chromagen labeling for steroid hormone receptors was imaged with light microscopy using a 10× objective, and ImageJ software was used to quantify the number of PR, ERα, or AR-positive nuclei within defined regions. Immunofluorescent labeling of steroid hormone receptors was imaged using confocal microscopy with a Plan Neofluar 20× objective.

In GnRH-GFP control and PNA mice, 10 GnRH neurons were selected at random from the rPOA. GnRH neurons were imaged using confocal microscopy with a Plan Neofluar 40× objective with 3× zoom function. The density of spines and closely apposed vGluT2- or vGaT-ir puncta was calculated at the GnRH neuron soma and within 15-μm segments of the dendrite for 75 μm (14). Close vGluT2- or vGaT-ir puncta were considered to contact GnRH neurons when no black pixels were seen between the green and red signal. In sections collected from vGaT-cre mice injected with Ad-iZ/EGFPf, the number of EGFPf-positive fibers contacting the GnRH neuron soma and within 15-μm segments of the dendrite for 75 μm was counted. The density of closely apposing EGFPf-positive fibers contacting the GnRH neuron was expressed as the number of fibers per μm of somal circumference and the number of fibers per μm of the dendrite. Lastly, the degree that ARN GABAergic fibers contacted GnRH neurons was calculated by defining the percentage of GnRH neurons contacted by ARN GABAergic fibers at a single point, multiple points, or in a bundling configuration.

Statistical Analysis. Statistical analysis was performed using PRISM software (GraphPad). Control and PNA groups were compared using a two-tailed t test. LH samples from the P4 negative feedback trial were compared using repeated measures two-way ANOVA with Tukey multiple comparisons posttests. The percentage of GnRH neurons contacted at single points, multiple points, or bundled with ARN GABA neurons in control and PNA mice was compared using a two-way ANOVA with Tukey posttest. All data are represented as a mean ± SEM. A P value of <0.05 was accepted as statistically significant. *$P < 0.05$, **$P < 0.01$, ***$P < 0.001$.

1. Herbison AE (2006) Physiology of the gonadotropin-releasing hormone neuronal network. *Knobil and Neil's Physiology of Reproduction*, ed Neill JD (Raven Press, New York), 3rd Ed, pp 1415–1482.
2. Azziz R, Marin C, Hoq L, Badamgarav E, Song P (2005) Health care-related economic burden of the polycystic ovary syndrome during the reproductive life span. *J Clin Endocrinol Metab* 90(8):4650–4658.
3. Padmanabhan V (2009) Polycystic ovary syndrome—"A riddle wrapped in a mystery inside an enigma". *J Clin Endocrinol Metab* 94(6):1883–1885.
4. McCartney CR, Eagleson CA, Marshall JC (2002) Regulation of gonadotropin secretion: Implications for polycystic ovary syndrome. *Semin Reprod Med* 20(4):317–326.
5. Burt Solorzano CM, et al. (2012) Neuroendocrine dysfunction in polycystic ovary syndrome. *Steroids* 77(4):332–337.
6. Pastor CL, Griffin-Korf ML, Aloi JA, Evans WS, Marshall JC (1998) Polycystic ovary syndrome: Evidence for reduced sensitivity of the gonadotropin-releasing hormone pulse generator to inhibition by estradiol and progesterone. *J Clin Endocrinol Metab* 83(2):582–590.
7. Pielecka J, Quaynor SD, Moenter SM (2006) Androgens increase gonadotropin-releasing hormone neuron firing activity in females and interfere with progesterone negative feedback. *Endocrinology* 147(3):1474–1479.
8. Robinson JE, Forsdike RA, Taylor JA (1999) In utero exposure of female lambs to testosterone reduces the sensitivity of the gonadotropin-releasing hormone neuronal network to inhibition by progesterone. *Endocrinology* 140(12):5797–5805.
9. Shi D, Vine DF (2012) Animal models of polycystic ovary syndrome: A focused review of rodent models in relationship to clinical phenotypes and cardiometabolic risk. *Fertil Steril* 98(1):185–193.
10. Abbott DH, Zhou R, Bird IM, Dumesic DA, Conley AJ (2008) Fetal programming of adrenal androgen excess: Lessons from a nonhuman primate model of polycystic ovary syndrome. *Endocr Dev* 13:145–158.
11. Xita N, Tsatsoulis A (2006) Review: Fetal programming of polycystic ovary syndrome by androgen excess: Evidence from experimental, clinical, and genetic association studies. *J Clin Endocrinol Metab* 91(5):1660–1666.
12. Hague WM, et al. (1990) The prevalence of polycystic ovaries in patients with congenital adrenal hyperplasia and their close relatives. *Clin Endocrinol (Oxf)* 33(4):501–510.
13. Barnes RB, et al. (1994) Ovarian hyperandrogynism as a result of congenital adrenal virilizing disorders: Evidence for perinatal masculinization of neuroendocrine function in women. *J Clin Endocrinol Metab* 79(5):1328–1333.
14. Moore AM, Prescott M, Campbell RE (2013) Estradiol negative and positive feedback in a prenatal androgen-induced mouse model of polycystic ovarian syndrome. *Endocrinology* 154(2):796–806.
15. Sullivan SD, Moenter SM (2004) Prenatal androgens alter GABAergic drive to gonadotropin-releasing hormone neurons: Implications for a common fertility disorder. *Proc Natl Acad Sci USA* 101(18):7129–7134.
16. Leranth C, et al. (1992) Transmitter content and afferent connections of estrogen-sensitive progestin receptor-containing neurons in the primate hypothalamus. *Neuroendocrinology* 55(6):667–682.
17. Thind KK, Goldsmith PC (1997) Expression of estrogen and progesterone receptors in glutamate and GABA neurons of the pubertal female monkey hypothalamus. *Neuroendocrinology* 65(5):314–324.
18. Dufourny L, Caraty A, Clarke IJ, Robinson JE, Skinner DC (2005) Progesterone-receptive dopaminergic and neuropeptide Y neurons project from the arcuate nucleus to gonadotropin-releasing hormone-rich regions of the ovine preoptic area. *Neuroendocrinology* 82(1):21–31.
19. Foradori CD, et al. (2002) Colocalization of progesterone receptors in parvicellular dynorphin neurons of the ovine preoptic area and hypothalamus. *Endocrinology* 143(11):4366–4374.
20. Roland AV, Moenter SM (2011) Prenatal androgenization of female mice programs an increase in firing activity of gonadotropin-releasing hormone (GnRH) neurons that is reversed by metformin treatment in adulthood. *Endocrinology* 152(2):618–628.
21. Wintermantel TM, et al. (2006) Definition of estrogen receptor pathway critical for estrogen positive feedback to gonadotropin-releasing hormone neurons and fertility. *Neuron* 52(2):271–280.
22. Sleiter N, et al. (2009) Progesterone receptor A (PRA) and PRB-independent effects of progesterone on gonadotropin-releasing hormone release. *Endocrinology* 150(8):3833–3844.
23. Skinner DC, et al. (1998) The negative feedback actions of progesterone on gonadotropin-releasing hormone secretion are transduced by the classical progesterone receptor. *Proc Natl Acad Sci USA* 95(18):10978–10983.
24. Yeo S-H, Herbison AE (2014) Estrogen-negative feedback and estrous cyclicity are critically dependent upon estrogen receptor-α expression in the arcuate nucleus of adult female mice. *Endocrinology* 155(8):2986–2995.
25. Vong L, et al. (2011) Leptin action on GABAergic neurons prevents obesity and reduces inhibitory tone to POMC neurons. *Neuron* 71(1):142–154.
26. Witham EA, Meadows JD, Shojaei S, Kauffman AS, Mellon PL (2012) Prenatal exposure to low levels of androgen accelerates female puberty onset and reproductive senescence in mice. *Endocrinology* 153(9):4522–4532.
27. Roland AV, Nunemaker CS, Keller SR, Moenter SM (2010) Prenatal androgen exposure programs metabolic dysfunction in female mice. *J Endocrinol* 207(2):213–223.
28. Diamanti-Kandarakis E, Dunaif A (2012) Insulin resistance and the polycystic ovary syndrome revisited: An update on mechanisms and implications. *Endocr Rev* 33(6):981–1030.
29. Steyn FJ, et al. (2013) Development of a methodology for and assessment of pulsatile luteinizing hormone secretion in juvenile and adult male mice. *Endocrinology* 154(12):4939–4945.
30. Cheong RY, Porteous R, Chambon P, Abrahám I, Herbison AE (2014) Effects of neuron-specific estrogen receptor (ER) α and ERβ deletion on the acute estrogen negative feedback mechanism in adult female mice. *Endocrinology* 155(4):1418–1427.
31. Chappell PE, Lydon JP, Conneely OM, O'Malley BW, Levine JE (1997) Endocrine defects in mice carrying a null mutation for the progesterone receptor gene. *Endocrinology* 138(10):4147–4152.
32. Foecking EM, Szabo M, Schwartz NB, Levine JE (2005) Neuroendocrine consequences of prenatal androgen exposure in the female rat: Absence of luteinizing hormone surges, suppression of progesterone receptor gene expression, and acceleration of the gonadotropin-releasing hormone pulse generator. *Biol Reprod* 72(6):1475–1483.
33. Cheng G, Coolen LM, Padmanabhan V, Goodman RL, Lehman MN (2010) The kisspeptin/neurokinin B/dynorphin (KNDy) cell population of the arcuate nucleus: Sex differences and effects of prenatal testosterone in sheep. *Endocrinology* 151(1):301–311.
34. Cottrell EC, Campbell RE, Han SK, Herbison AE (2006) Postnatal remodeling of dendritic structure and spine density in gonadotropin-releasing hormone neurons. *Endocrinology* 147(8):3652–3661.
35. Sorra KE, Harris KM (2000) Overview on the structure, composition, function, development, and plasticity of hippocampal dendritic spines. *Hippocampus* 10(5):501–511.
36. Herbison AE, Moenter SM (2011) Depolarising and hyperpolarising actions of GABA(A) receptor activation on gonadotrophin-releasing hormone neurones: Towards an emerging consensus. *J Neuroendocrinol* 23(7):557–569.
37. Sullivan SD, Moenter SM (2005) GABAergic integration of progesterone and androgen feedback to gonadotropin-releasing hormone neurons. *Biol Reprod* 72(1):33–41.
38. Johnston CA, Crawford PM (2014) Anti-epileptic drugs and hormonal treatments. *Curr Treat Options Neurol* 16(5):288.
39. Verrotti A, et al. (2011) Antiepileptic drugs, sex hormones, and PCOS. *Epilepsia* 52(2):199–211.
40. Soper BD, Weick RF (1980) Hypothalamic and extrahypothalamic mediation of pulsatile discharges of luteinizing hormone in the ovariectomized rat. *Endocrinology* 106(1):348–355.
41. Navarro VM, et al. (2009) Regulation of gonadotropin-releasing hormone secretion by kisspeptin/dynorphin/neurokinin B neurons in the arcuate nucleus of the mouse. *J Neurosci* 29(38):11859–11866.
42. Goodman RL, et al. (2011) Evidence that the arcuate nucleus is an important site of progesterone negative feedback in the ewe. *Endocrinology* 152(9):3451–3460.
43. Goodman RL, et al. (2004) Evidence that dynorphin plays a major role in mediating progesterone negative feedback on gonadotropin-releasing hormone neurons in sheep. *Endocrinology* 145(6):2959–2967.
44. Campbell RE, Gaidamaka G, Han S-K, Herbison AE (2009) Dendro-dendritic bundling and shared synapses between gonadotropin-releasing hormone neurons. *Proc Natl Acad Sci USA* 106(26):10835–10840.
45. Spergel DJ, Krüth U, Hanley DF, Sprengel R, Seeburg PH (1999) GABA- and glutamate-activated channels in green fluorescent protein-tagged gonadotropin-releasing hormone neurons in transgenic mice. *J Neurosci* 19(6):2037–2050.
46. Vidal A, Zhang Q, Médigue C, Fabre S, Clément F (2012) DynPeak: An algorithm for pulse detection and frequency analysis in hormonal time series. *PLoS ONE* 7(7):e39001.

Moore et al.

NEUROSCIENCE

www.manaraa.com